



Experimental Investigation of Tribological and Rheological Behaviour of Hybrid Nanolubricants for Applications in Internal Combustion Engines

José M. Liñeira del Río^{1,2} · Ramón Rial³ · Khodor Nasser¹ · María J. G. Guimarey^{1,4}

Received: 12 November 2022 / Accepted: 22 January 2023 / Published online: 9 February 2023
© The Author(s) 2023

Abstract

In this study, the improvement in SAE 10W-40 engine oil tribological performance after the addition of magnesium oxide (MgO) nanoadditive and two different phosphonium-based ionic liquids (ILs) was investigated. Besides, the rheological behaviour of MgO-based nanolubricant and IL-based hybrid nanolubricants at the temperature range from 293.15 to 363.15 K was studied. The nanoparticle characterization was performed by means of transmission electron microscopy (TEM), Fourier-transform infrared spectroscopy (FTIR), Raman spectroscopy, X-ray diffraction (XRD) and scanning electron microscopy (SEM). The tribological properties, friction coefficients and wear parameters of the formulated oil modified with 0.01 wt% MgO and 1 wt% ILs compared with the neat 10W-40 oil were performed and analysed using a ball-on-three-pins tribometer and a 3D optical profilometer, respectively. Further analysis on the worn surface was shown by Raman spectroscopy and SEM images illustrating the formation of the protective IL and MgO tribo-films as hybrid additives. In friction tests with sliding steel-steel tribo-pairs, IL3-based hybrid nanolubricant decreased the coefficient of friction and wear volume by 7% and 59%, respectively, in comparison with the neat SAE 10W-40, hence better positive synergies were found for MgO and IL3 as hybrid additives. Interestingly, the thermophysical characterization by rheology also revealed that the nanoparticle and ionic liquids addition did not affect neither the viscosity response nor the Newtonian behaviour of the engine oil, adequately meeting the requirements for their use in internal combustion engines.

✉ María J. G. Guimarey
mariajesus.guimarey@usc.es

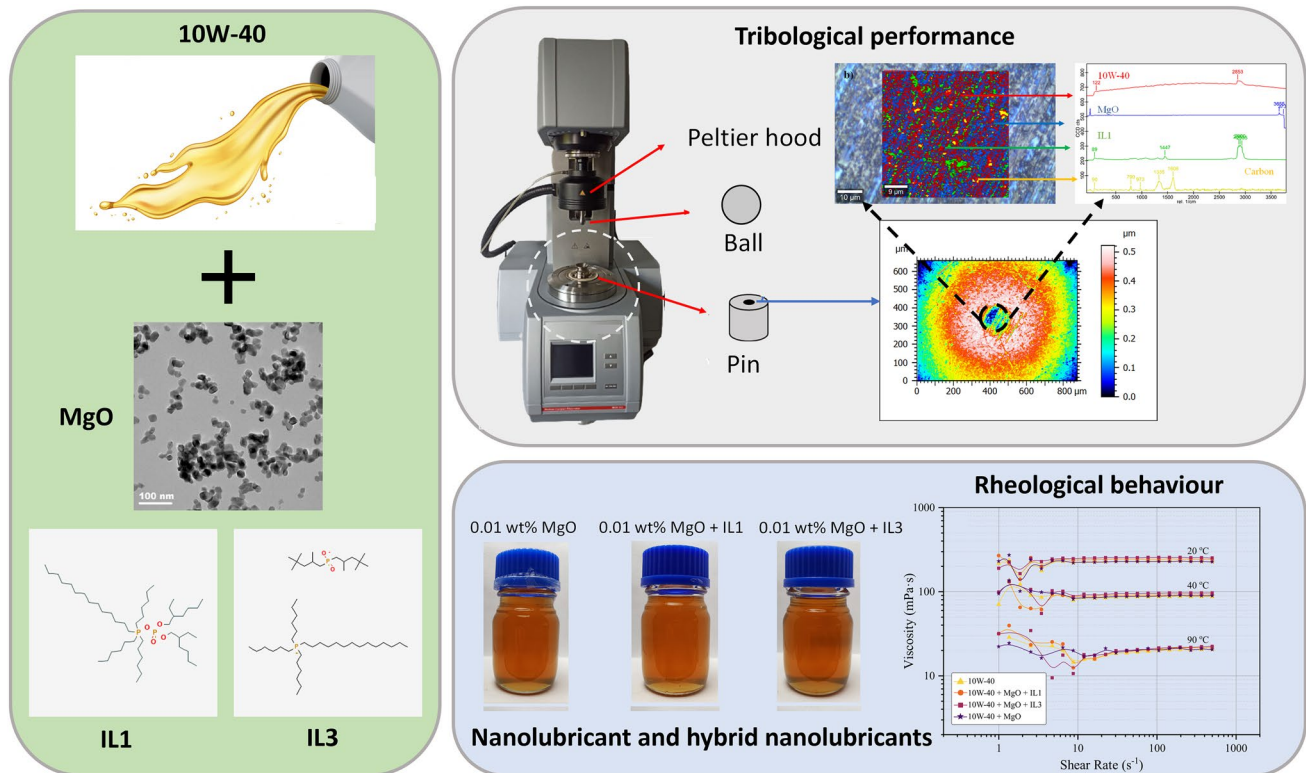
¹ Laboratory of Thermophysical and Tribological Properties, Nafomat Group, Department of Applied Physics, Faculty of Physics, University of Santiago de Compostela, 15782 Santiago de Compostela, Spain

² FEUP, Universidade do Porto, Rua Dr. Roberto Frias S/N, 4200-465 Porto, Portugal

³ Soft Matter and Molecular Biophysics Group, Department of Applied Physics, University of Santiago de Compostela, 15782 Santiago de Compostela, Spain

⁴ Department of Design and Engineering, Faculty of Science & Technology, Bournemouth University, Talbot Campus, Poole BH12 5BB, UK

Graphical Abstract



Keywords Lubricant · Nanoparticles · Phosphonium-based ionic liquids · Tribological mechanisms · Rheology

1 Introduction

In automotive engines, the high frictional energy loss between the tribo-pairs especially at the piston rings and cylinder liner surface contact was estimated to be from 20 to 30% of its total power loss [1]. This matter has led researchers to investigate various additives as possible components of conventional lubricating oil. A multifunctional engine lubrication system is considered more critical and effective since it could have various characteristics to reduce friction, attenuate wear, enhance heat transfer capabilities, inhibit corrosion and oxidation and remove wear debris and contamination, simultaneously. Thus, engine oil plays a key role in an internal combustion engine to achieve greater fuel economy by reducing friction and wear of the interacting surfaces [2]. Due to certain limitations of the base oils physicochemical properties as to fulfil the desired requirements, a further improvement is required in order to enhance their performance. Recently, research has focused on the use of nanomaterials to improve the lubricity and durability

of commercial oils which plays a key role in the wear and friction processes of materials [3–6]. Thus, nanolubricants can enable major technological breakthroughs and cost savings in a variety of domestic and industrial applications, including transport, electronic devices, chemical engineering applications, aerospace, wind turbines and automotive [5].

In addition, viscosity is considered a significant thermo-physical characteristic that also influences lubricant performance. The flow behaviour of fluids is determined by viscosity variations with shear rate, shear stress and temperature [7]. Moreover, a fluid is considered to be Newtonian if shear stress changes linearly with shear rate, and non-Newtonian if its response depends on the movement. In terms of viscosity, it means that in a Newtonian fluid its viscosity will remain constant regardless of the applied forces. An optimum viscosity range ensures proper lubricant film formation and therefore effective lubrication, so it is crucial not to alter this property outside the operating range for a given application.

The tribological and rheological properties of lubricants are the main factors to be considered to prevent wear under operating conditions. The addition of nano-sized spherical particles can improve these properties, making the lubricating oil performance stable under severe operating conditions; however, the selection of suitable nanoparticles is

very important [8]. Friction and wear behaviour of nanoparticles content are associated with hardness, size and deposition efficiency of nanoparticles on worn surfaces [9]. Much work has been done on organic and inorganic nanoparticles for application as extreme pressure (EP) and anti-wear agents [2, 10, 11]. Among all of them, the metal oxides are commonly used as additives for anti-friction and anti-wear applications, and they can be composed of a variety of diverse materials, including titanium, copper, zirconium, zinc, cerium, aluminium and iron oxides. Wu et al. [12] have studied the behaviour of two different metal oxides, TiO_2 and CuO , as nanoadditives in two lubricating oils, API-SF engine oil (SAE30 LB51153) and a base oil (SAE30 LB51163-11), revealing a decrease in the friction of both lubricants when these nanoadditives were added, in particular for CuO nanolubricants. Hernández Battez et al. [13] have discussed the tribological behaviour of CuO , ZrO_2 and ZnO nanoparticles as anti-wear additives of a polyalphaolefin (PAO6), concluding that all nanolubricants reduce the friction coefficient and increase the anti-wear ability of base oil (PAO6). The mechanism by which the lubricating behaviour for the nanolubricants is based on metal oxides (Al_2O_3 , SiO_2 , CuO , ZnO , ZrO_2 and TiO_2) is improved and based on the formation of a layer formed by mechanical compaction [12, 14–16]. Among the wide variety of existing nanoparticles, magnesium oxide has better properties than many of them, as it is easily soluble and has lower density [17]. However, MgO has only recently been studied for tribological purposes by Singh et al. [17] and Loo et al. [18], demonstrating excellent anti-wear results, reducing wear rate by almost 50% in vegetable oil and 7% of wear scar diameter in biofuel, respectively. These outstanding tribological

Fig. 1 Raman spectrum of 10W-40 formulated oil

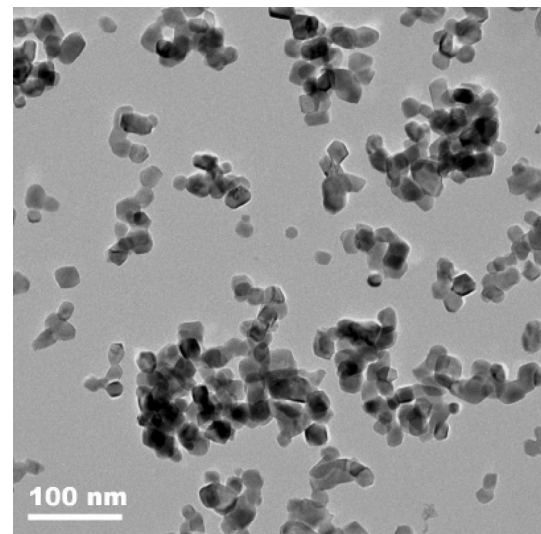
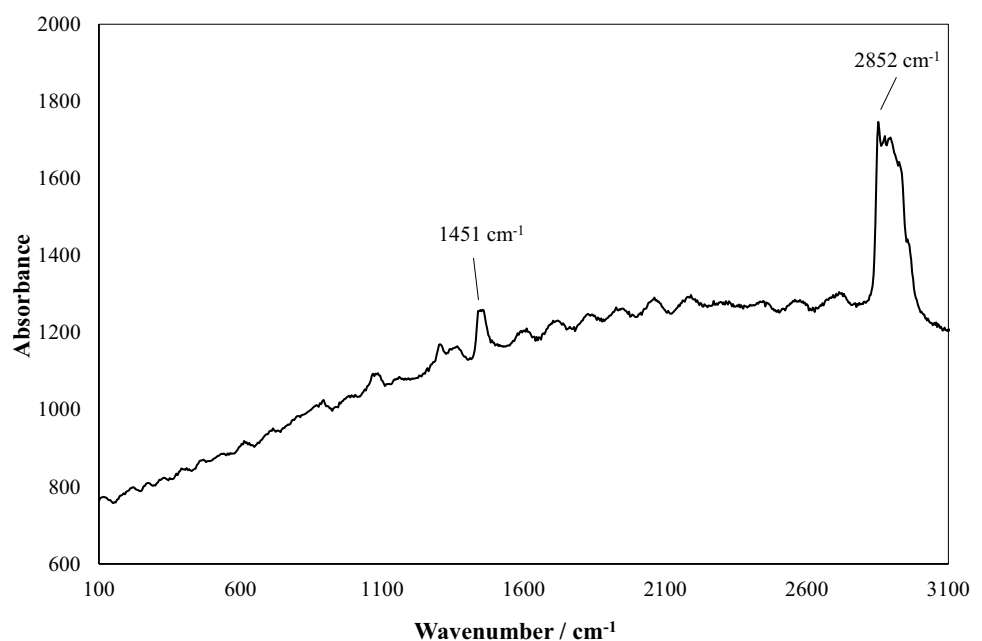


Fig. 2 Transmission electron microscopy (TEM) image of MgO nanoparticles [34]

results were obtained using MgO concentrations of 0.2, 0.6 and 1.2 [17] and 0.1 and 0.2 [18], respectively. The use of low concentrations of additives in engine oils is more effective in reducing the coefficient of friction in piston rings and cylinder lines [19]. Therefore, the need to further study the ability of MgO at low concentrations as a lubricant additive is of great interest.

However, a main challenge in this field is the stability of nanoadditives in oils along time, being a vital matter that affects the nanolubricant lubrication performance [20]. A way to elongate stability and avoid agglomerates in

Fig. 3 Infrared spectrum of MgO nanopowders

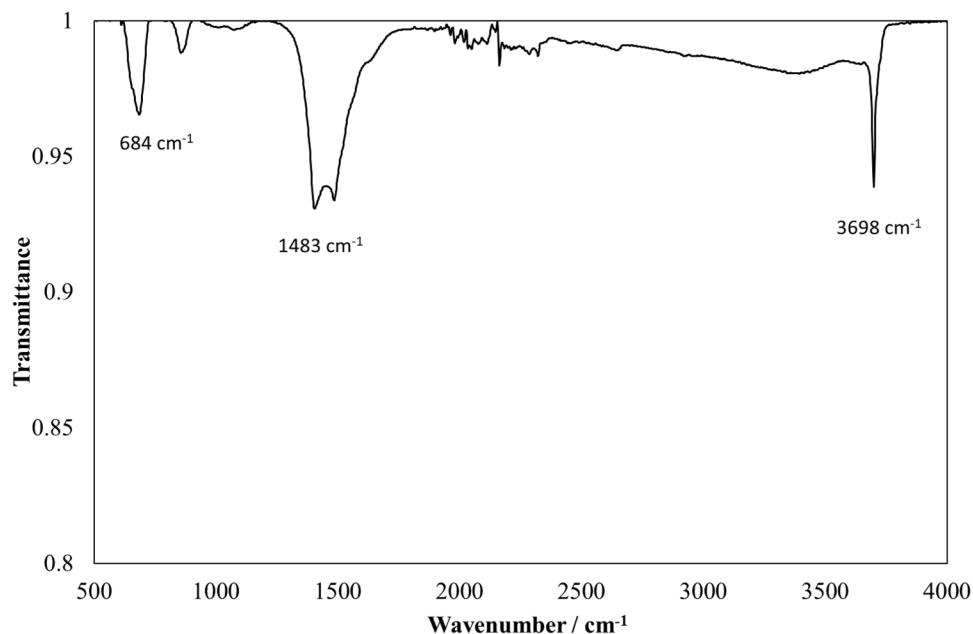
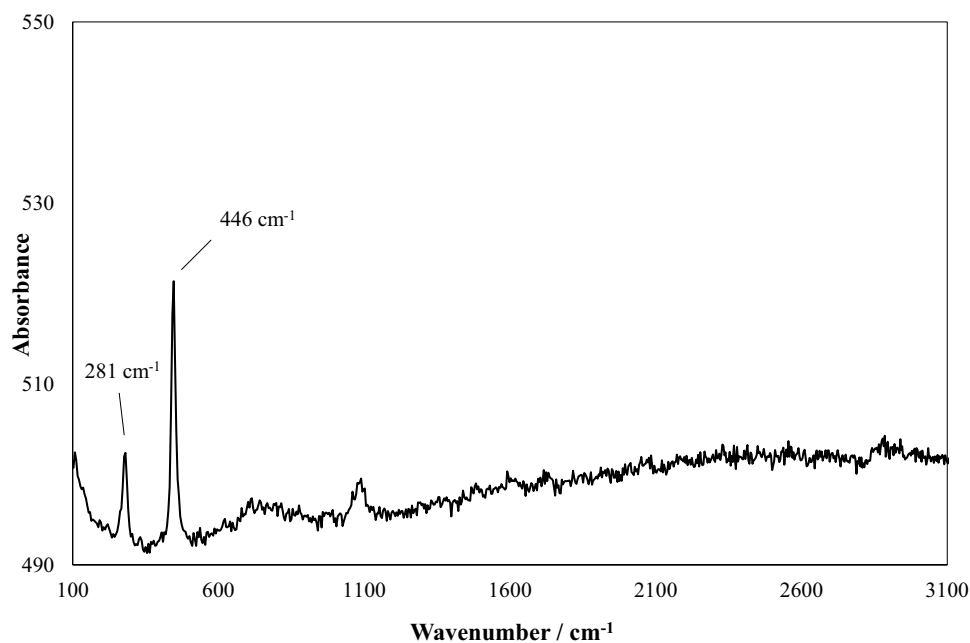
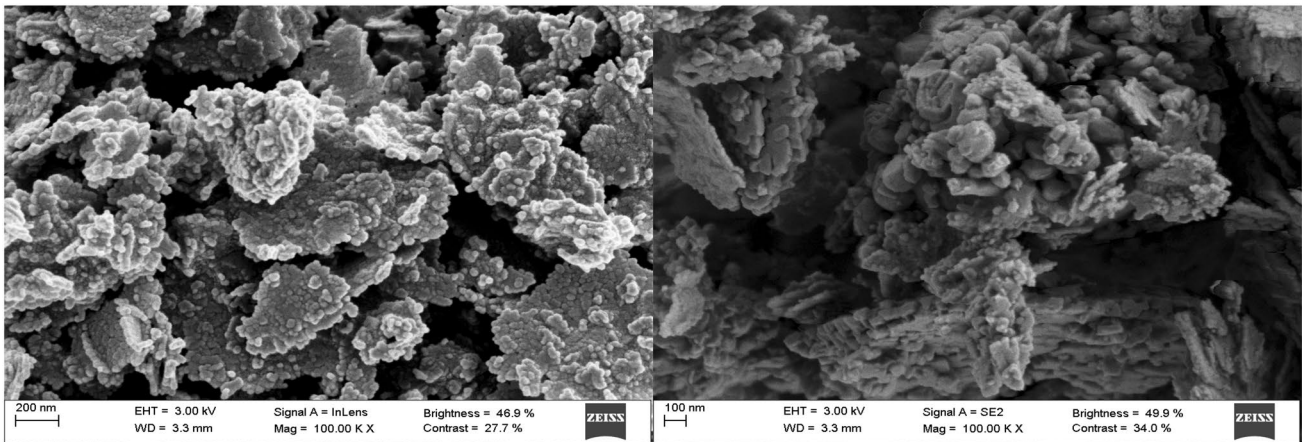
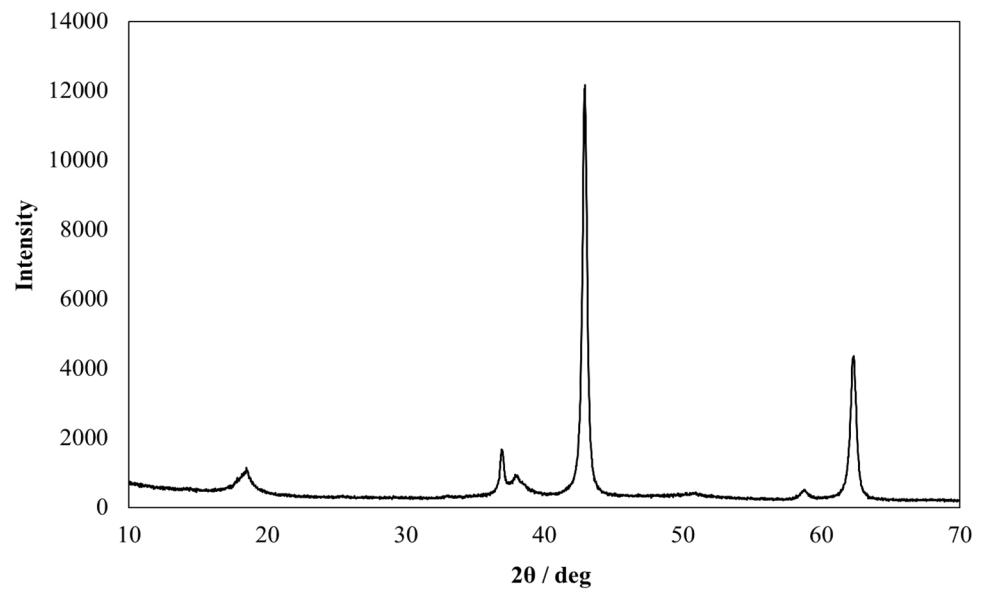


Fig. 4 Raman spectrum of MgO nanopowders



nanolubricants as in other nanofluids is the use of coated nanoparticles and organic or hybrid nanomaterials [21, 22]. Another alternative to improve the stability of the nanoadditives in the lubricant is the addition of surfactants as ionic liquids (ILs). ILs are excellent dispersants for the stabilization of well-characterized nanomaterials. ILs are molten salts at room temperature that possess unique physicochemical properties and have shown good oil-soluble and excellent lubricating properties, especially protic ILs with long alkyl

chains [23–26]. Among the myriad of existing protic ILs, phosphonium cation-based ILs exhibit outstanding solubility in non-polar liquids, thus facilitating their use as ILs in conventional lube oils [27]. Since the International Lubricants Standardization and Approval Committee specification (ILSAC GF-5) restricts the phosphorus content to a range of 0.06–0.08 wt% [28], considering the molecular weight of phosphonium ILs, previous work has used a concentration of 1 wt% of these ILs in engine lubricants [24, 28, 29]. The

Fig. 5 XRD pattern of MgO nanopowders**Fig. 6** SEM images MgO nanopowders

double action in the case of IL-modified hybrid nanoadditives reveals that nanomaterials are beneficial for increasing wear resistance due to their good mechanical strength, and ILs can improve their dispersion in lubricating oils [26].

This work focuses on the study of the synergistic effects of metal oxide nanoparticles, magnesium oxide (MgO), with two phosphonium ionic liquids on the tribological and rheological behaviour of a 10W-40 commercial engine oil. In previous studies, the application of a commercial engine oil with the effect of MgO combined with ionic liquids has never been considered for tribological applications. Most of the studies have reported the rheological behaviour by using MWCNT (COOH-functionalized)/MgO as lubricant additives to engine oils [30, 31]. The authors have performed this study and found better results that are beneficial to the readers of this journal.

2 Materials and Methods

2.1 Oil, Nanoadditive and Ionic Liquids

Commercial SAE 10W-40 oil was used as the base oil to prepare the nanolubricant and hybrid nanolubricants in this work. 10W-40 oil, supplied by Repsol, is a semi-synthetic oil characterized by being a mixture of mineral and synthetic oils. This engine oil has a density, ρ , of 0.8498 g cm⁻³ at 298.15 K, a kinematic viscosity, ν , of 96.45 and 14.54 mm² s⁻¹ at 303.15 and 373.15 K, respectively, and a viscosity index, VI, of 162. 10W-40 has several advantages over other types of oils such as improving the engine performance, increasing its lifespan and keeping it more viscous, which means that it is a cleaner oil than others. Furthermore, it is considered less expensive than synthetic oils.

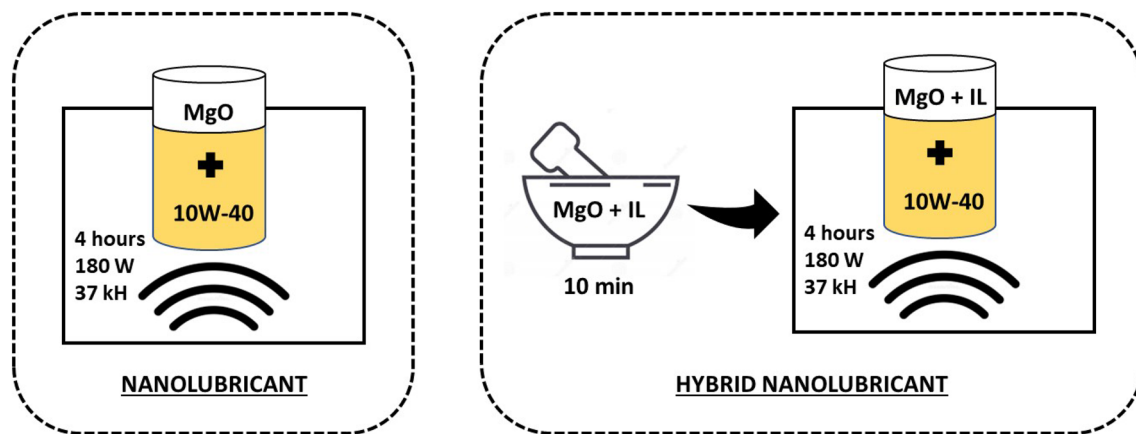


Fig. 7 Nanolubricant preparation scheme

Raman spectrum of formulated 10W-40 oil was performed with a WITec alpha300R + confocal Raman microscopy at a wavelength of 532 nm. Raman spectrum of 10W-40 is shown in Fig. 1, which detects an intense band around $2800\text{--}3000\text{ cm}^{-1}$ with a peak of 2852 cm^{-1} corresponding to C–H stretching [32] and other peak at 1451 cm^{-1} that corresponds to $\delta(\text{CH}_3)$ vibrations [33].

Concerning the additives, magnesium (II) oxide (MgO) nanoparticles, CAS:1309-48-4, $\sim 30\text{ nm}$ size, 99.9% purity, were supplied by Iolitec. Transmission electron microscopy (TEM) was provided by the manufacturer to determine the nanoparticle average particle size. Figure 2 confirms the average particle size of 30 nm .

In addition, these nanopowders were characterized by means of different techniques, such as Infrared (FTIR), Raman spectroscopy and X-ray diffraction (XRD). As can be observed in Fig. 3, FTIR reveals at 684 cm^{-1} the stretching vibration mode of Mg–O–Mg bonds, the bending vibration of surface hydroxyl group at 1483 cm^{-1} and the presence of hydroxyl group at 3698 cm^{-1} [35–37].

Raman spectroscopy shows the presence of two characteristic bands at 281 and 446 cm^{-1} (Fig. 4). The first one is related to a TA phonon in the boundary zone while the latter one corresponds with a TA phonon at the centre zone, being T: transversal (in-plane) waves and A: acoustic modes. The found Raman lines are closely paired with previous characterizations of MgO [38, 39].

X-ray diffraction, XRD, method was employed to find the crystalline nature of MgO nanoparticles, for this aim a Bruker D8 Advance was utilized. XRD analysis (Fig. 5) shows important peaks at angles 36.99° , 42.94° and 62.33° associated with (1 1 1), (0 0 2) and (2 0 2) planes (JCPDS No. 87-0653) that suggests the existence of a cubic polycrystalline structure for MgO nanoparticles [35]. Additionally, the XRD pattern exhibits a high strong (0 0 2)

orientation peak displaying a high crystallinity of MgO nanoparticles [35].

Scanning electron microscopy studies (SEM) were performed to get clear information of MgO nanoparticles morphology and shape. Figure 6 displays the surface topography of nanoparticles, observing that they are spherical, uniform in size and with agglomeration [40, 41].

The ionic liquids used as lubricant additives were trihexyltetradecylphosphonium bis(2-ethylhexyl) phosphate,

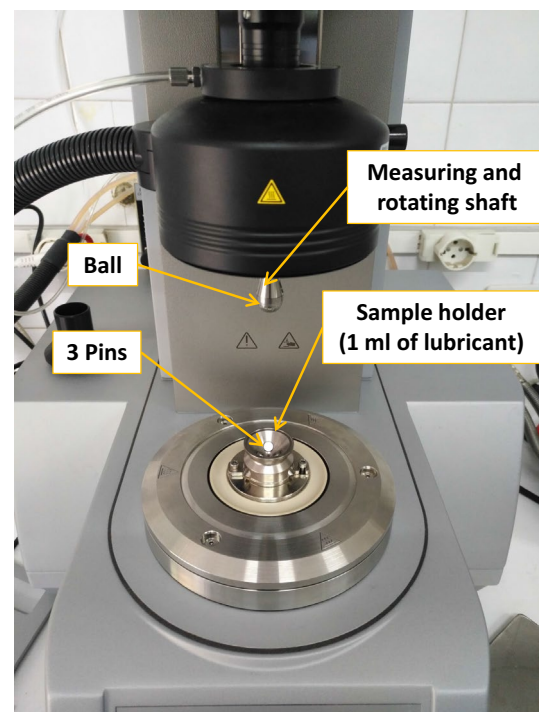


Fig. 8 Tribology cell T-PTD200 in combination with a Peltier hood H-PTD 200 mounted on MCR 302 rheometer the experimental test setup

[P_{6,6,6,14}][DEHP], (IL1, CAS number: 1092655-30-5 and purity > 0.98), and trihexyltetradecylphosphonium bis(2,4,4-trimethylpentyl) phosphinate, [P_{6,6,6,14}][(iC8)₂PO₂], (IL3, CAS number: 465527-58-6 and purity > 0.9), both were supplied by Iolitec and previously characterized by Nasser et al. [29].

2.2 Formulation of Nanolubricant and Hybrid Nanolubricants

An engine oil-based nanolubricant was prepared with a concentration of 0.01 wt% of MgO nanopowders. A low concentration of MgO was selected to interpret its effect on friction and consequently wear rather than high concentrations as in previous performed studies [17, 18]. Hybrid nanolubricants were prepared with the same MgO concentration and 1 wt% of two different ionic liquids: trihexyltetradecylphosphonium bis(2-ethylhexyl)phosphate (IL1) or trihexyltetradecylphosphonium bis(2,4,4-trimethylpentyl) phosphinate (IL3) dispersed in the commercial oil 10W-40. The concentration of 1 wt% of each ionic liquid was selected on the basis of the maximum permitted phosphorus content, which has been used in previous studies [24, 25]. Therefore, the subsequent nanolubricant and hybrid nanolubricants were formulated: 10W-40 + 0.01 wt% MgO, 10W-40 + 0.01 wt% MgO + 1 wt% IL1 and 10W-40 + 0.01 wt% MgO + 1 wt% IL3.

The formulation scheme of the nanolubricant and hybrid nanolubricants is shown in Fig. 7. For the nanolubricant, a traditional two-step process was employed: dry MgO nanopowders were added to the 10W-40 oil after reaching the desired mass concentration using a Sartorius balance, with a readability of 0.01 mg. Afterwards, the homogenization of the oil and the nanopowders (nanolubricant) was performed by an ultrasound bath (Fisherbrand) for a duration of 4 h continuously, at 180 W power and 37 kHz frequency. Concerning the hybrid nanolubricant with MgO and IL, an improved two-step method was used [29, 42, 43], as a replacement for the directly mixing nanoparticles with oil. For this purpose, suitable quantities of MgO nanoadditives were set in an agate mortar and mechanically mixed with the appropriate quantity of ILs for 10 min with no stop to get a final prepared mixture of MgO and IL. Indeed, the lubricity of the IL is governed by the structure of the anion [44] which is in this case [DEHP] for IL1 and [(iC8)₂PO₂] for IL3. The method used might enhance the lubricity of the ILs by introducing the nanoadditives MgO separately with continuous mixing before its addition as hybrid additive to 10W-40 oil. This technique obtains more stable mixture, instead of individual addition of IL and MgO. Subsequently, this mixture was added to the 10W-40 oil and homogenized using an ultrasonic bath, similarly as in the preceding process. Two sets of the prepared sample were made: one to

study the stability against time and the other one to perform friction tests.

2.3 Friction Tests and Wear Analysis

Tribological tests of the neat oil (10W-40), the nanolubricant (with MgO) and the hybrid nanolubricants (with MgO/ILs) were performed with a MCR 302 rheometer from Anton Paar (Graz, Austria) coupled with a tribology cell T-PTD200 equipped by a Peltier hood H-PTD200 for temperature control, being the tribological configuration ball-on-three pins. In this configuration, the ball (upper specimen) is mounted on a vertical shaft that is driven by the rheometer motor, while the three pins (lower specimens) are set inside a holder at a 45° angle of contact to the rotating shaft. To fully cover the top level of the pins mounted into the sample holder, around 1 ml of tested lubricant was added. Through every tribological trial, the ball rotates against the three pins under a static force applied by the rheometer. This axial force is relocated into three normal forces acting perpendicularly to the surfaces of the pins [45]. Figure 8 shows the real tribometer with the T-PTD200 tribo cell; more details about the tribometer can be seen in a previous research [29]. The specimens used were polished AISI 52100 (100Cr6) steel balls (Ra = 20 nm) and pins (Ra = 50 nm) with hardness of 62–66 HRC. AISI 52100 steel is one of the most widely used materials in bearings [46], one of the components of internal combustion engines where significant mechanical power losses occur [47]. Regarding the test conditions, 213 rpm rotational speed (0.1 m s⁻¹), under 20 N axial load (9.43 N in each pin) implying a maximum Hertzian pressure of 1.1 GPa, sliding distance of 340 m, sliding time of 3500 s and optimum operating temperature for internal combustion engines temperature of 363.15 K were chosen. Three trials were performed for each friction test to obtain accurate experimental average values.

Concerning the wear evaluation produced on the surfaces of the pins during the aforementioned friction tests, a high-resolution 3D profiler S Neox Sensofar was employed to quantify the generated wear scar through different wear parameters, such as wear track width (WTW), wear track depth (WTD), wear area and volume. Wear measurements were taken in confocal mode using a 10× objective and the SensoMAP software, integrated with the profilometer, which provides a fast and accurate analysis of the surface geometry. By means of these wear measurements for all the tests (with base oil, nanolubricant and hybrid nanolubricants) a good comparison of the wear produced by the nano- and hybrid nanolubricants with respect to the formulated oil without nanoadditives and/or ILs can be determined. Regarding the measurements of the worn area, the 3D profiler first generates a cross-sectional profile of the worn surface and then the software determines the area as the subtraction of the worn

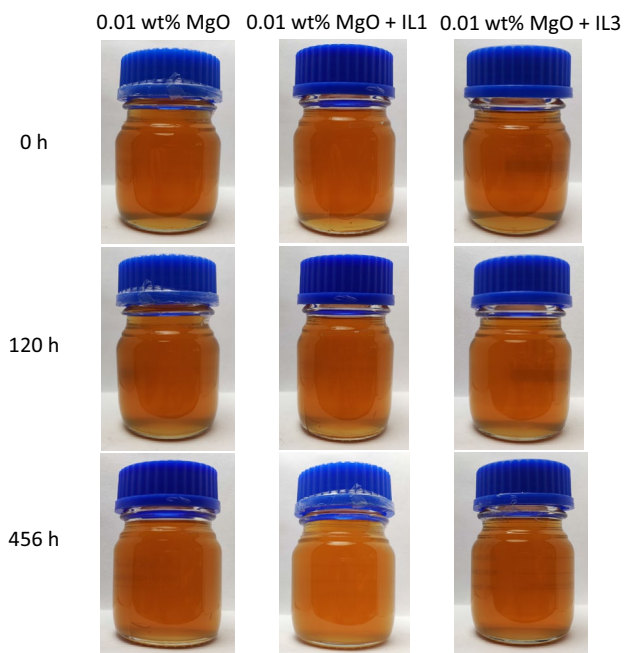


Fig. 9 Visual stability of 10W-40 nanolubricants with and without ILs

area (valley) minus the sum of the areas of the displaced material profiles on both sides of the worn track (peaks). The wear volume was automatically determined by the SensoMAP software by pre-setting the level of the unworn surface of the pin, and the software detects the coordinates of the points of the wear surface profile and calculates the volume of the hole below this level. The 3D profiler was also utilized to evaluate the worn track roughness (R_a) on

the surface of the pins used in tribotests to illustrate the anti-wear skill of each nano- and hybrid nanolubricant. For this reason, ISO4287 standard was applied using a Gaussian filter (cut-off: 0.08 mm wavelength). In addition, a Raman microscope WITec alpha300R+ was used to examine the internal worn track surface of the pins and acquire information about the nanolubricant and hybrid nanolubricants components (10W-40, MgO nanoparticles and ILs) and their distribution inside the worn scar as well as the tribological mechanisms occurred to discuss their influence in enhancing the tribological properties compared to the based oil.

To better understand the anti-wear mechanisms of the nanoparticles in the engine oil, the wear scar of the tested steel pins was also scanned and analysed by using FESEM Ultra plus model from ZEISS. An InLens secondary electron detector was used to record the SEM images at 3 kV. The equipment works in ultra-high vacuum, so the sample is metallized with Iridium (Ir), to avoid charging, in this case a thickness of 10 nm is deposited. To determine the composition of the surface of the sample, the EDX detector model INCA-X act of the commercial company OXFORD was used, all controlled with the AZtec software, the acquisition conditions are 20 kV and a working distance (WD) of 8.5 mm. These are the optimal conditions for capturing and collecting beads for a more accurate analysis.

2.4 Rheological Measurements

Rheological measurements were performed with the previous Anton Paar Rheometer Physica MCR 302 (Graz,

Fig. 10 Temporal evolution of the refractive index, n , at $T=293.15$ K for engine oil (10W-40), for nanolubricant and for hybrid nanolubricants

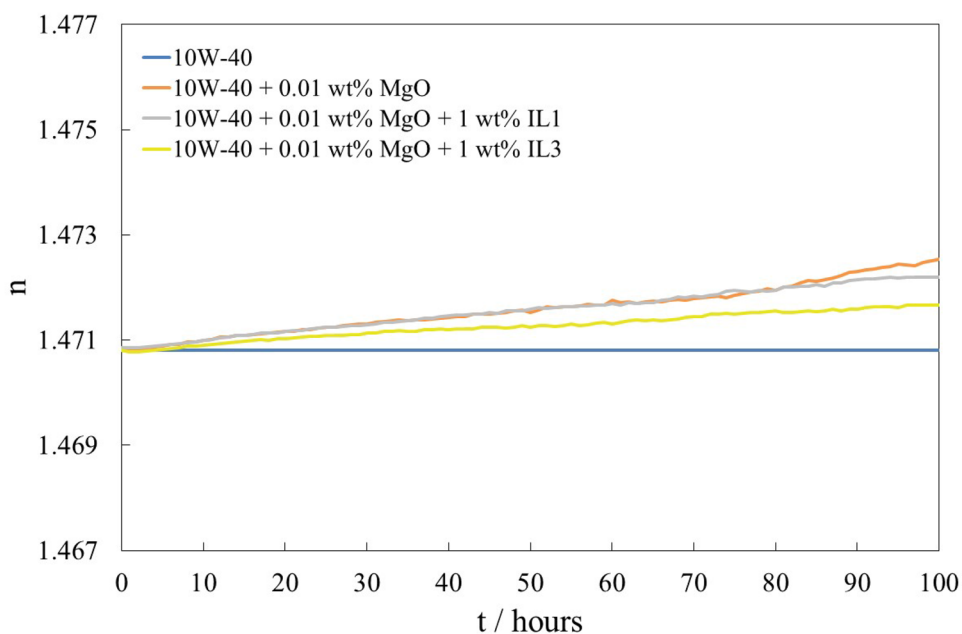


Fig. 11 Comparison between friction coefficients (μ) and wear volume reduction reached with 10W-40, IL-lubricants, MgO nanolubricant and hybrid nanolubricants

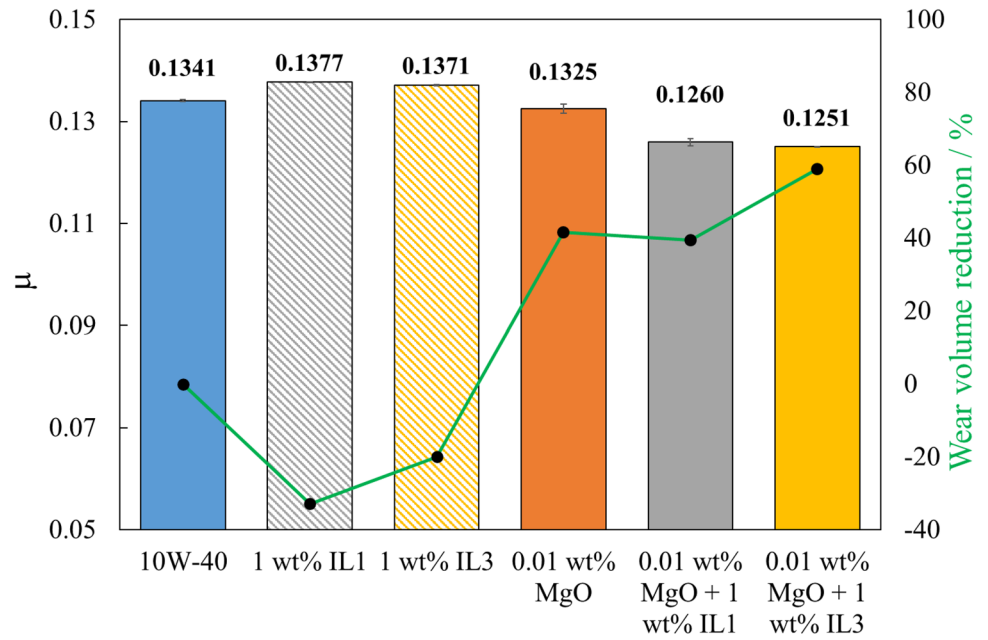
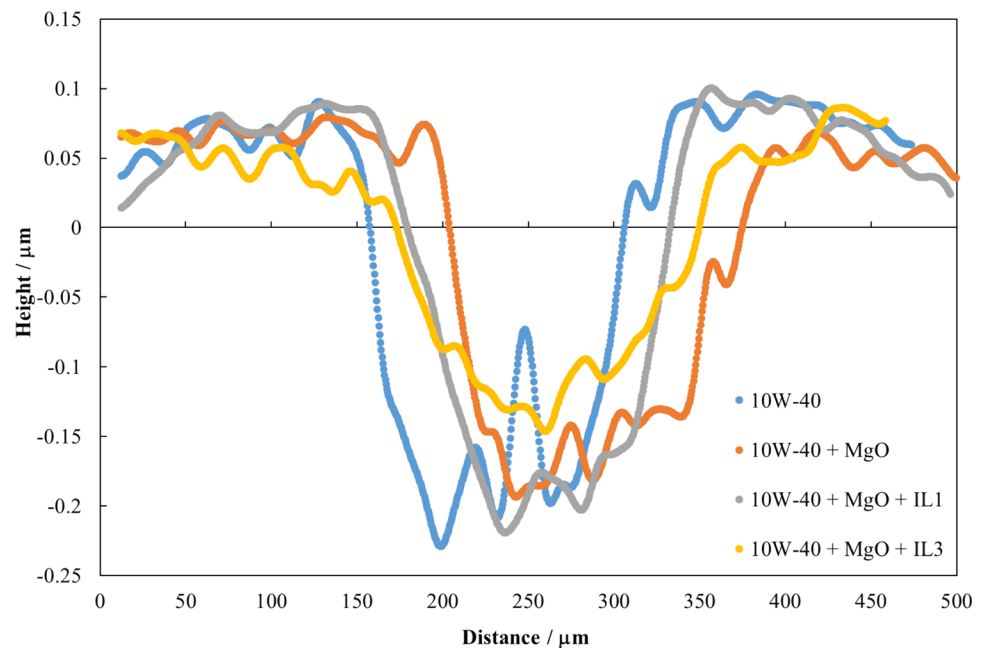


Table 1 Average friction coefficients, μ , as well as average wear parameters: width (WTW), depth (WTD), area and volume and their standard deviations for the analysed lubricants

Lubricant	μ	σ	WTW/mm	σ /mm	WTD/mm	σ /mm	Area/ mm ²	σ /10 ² mm ²	Volume/mm ³	σ /mm ³
10W-40	0.1341	0.0002	234	10	0.323	0.040	35.38	4.90	2347.7	200.1
+ 1 wt% IL1	0.1377	0.0001	242	5	1.082	0.040	80.52	1.98	3119.6	181.1
+ 1 wt% IL3	0.1371	0.0001	236	4	0.553	0.029	64.79	5.27	2816.8	152.4
+0.01 wt% MgO	0.1325	0.0009	199	20	0.245	0.031	28.29	4.38	1369.3	188.0
+0.01 wt% MgO+ 1 wt% IL1	0.1260	0.0007	201	13	0.253	0.050	29.90	5.29	1422.5	222.7
+0.01 wt% MgO+ 1 wt% IL3	0.1251	0.0001	219	14	0.220	0.019	26.83	3.67	962.0	86.3

Fig. 12 Cross section profiles comparison of worn tracks for the 10W-40 oil and the developed lubricants



Austria). The geometry chosen for the tests was a system of parallel plates of 25 mm diameter. To avoid unwanted dehumidification and to control temperature, a humidity chamber and a Peltier cell were used. Throughout the experiments, the gap was kept constant at 0.5 mm. Finally, an equilibration time of 5 min was set before the start of each test to minimize differences in temperature and firmness. Viscosity data were collected for a range of shear rates extending from 1 to 500 s⁻¹. Each data point corresponds to an average of three different readings. The experiments were conducted using neat 10W-40 engine oil, 0.01 wt% of MgO dispersed in the 10W-40 oil, and two different ionic liquids (IL1 and IL3) added to the MgO nanolubricant. Each of these conditions was repeated at three different temperatures: 293.15, 313.15 and 363.15 K.

3 Results, Analysis and Discussion

3.1 Stability of Nanolubricant and Hybrid Nanolubricants

The temporal stability of the MgO-based lubricants was estimated by visually examining the deposit of nanoparticles during time. Figure 9 proves that for all nano and hybrid nanolubricants there is no sedimentation earlier to three weeks after their preparation. This stability is much extended than that required to carry out the tribological and rheological testing (around 4 h per each designed lubricant).

The temporal evolution of the refractive index can be observed in Fig. 10. An overall refractive index variation of 0.092% and 0.058% over 100 h was obtained for IL1-based and for IL3-based hybrid MgO nanolubricants, respectively. The overall variation of the refractive index is smooth ($\leq 0.1\%$) during the 100 first hours after sonication for hybrid nanolubricant while a variation of 0.118% is reached at 100 h for the MgO nanolubricant. A better stability for the IL3 hybrid nanolubricants is verified. These results reveal that samples are stable during this time interval.

3.2 Friction and Wear

Figure 11 and Table 1 present the average friction coefficients (μ) for the MgO-based nanolubricants (with and without ILs), for IL-based lubricants (without MgO), and for the 10W-40 oil. It is evidently noted that the friction coefficient is reduced for both hybrid nanolubricants compared to that of 10W-40 oil. The possible improvements in the tribological behaviour of 10W-40 by the addition of both MgO NPs and ILs as hybrid additives are due to the double action of these additives at the surface of contact, instead of their individual addition, and the traditional

performance where MgO NPs could aid in polishing mechanisms and ILs in tribo-film formation. In particular, the greatest anti-friction performance occurred for the hybrid nanolubricant 10W-40 + 0.01 wt% MgO + 1 wt% IL3, presenting a friction coefficient of 0.125 versus 0.134 achieved for the commercial lubricant 10W-40 (Table 1), leading to a 7% friction reduction. In contrast, the addition of the ILs alone, without the presence of MgO nanoparticles, revealed an increase in the coefficient of friction with respect to commercial motor oil, with increases of 3% and 2% when IL1 and IL3 were used, respectively. This fact reveals that the improved tribological performance is not due to the ionic liquid itself. However, with the individual addition of magnesium oxide nanoparticles without any ionic liquid, the coefficient of friction showed almost slight reduction (0.132). This is evidence that a positive synergy between ILs and MgO nanoparticles takes place, as their tribological behaviour on engine oil separately is not the same as when combined.

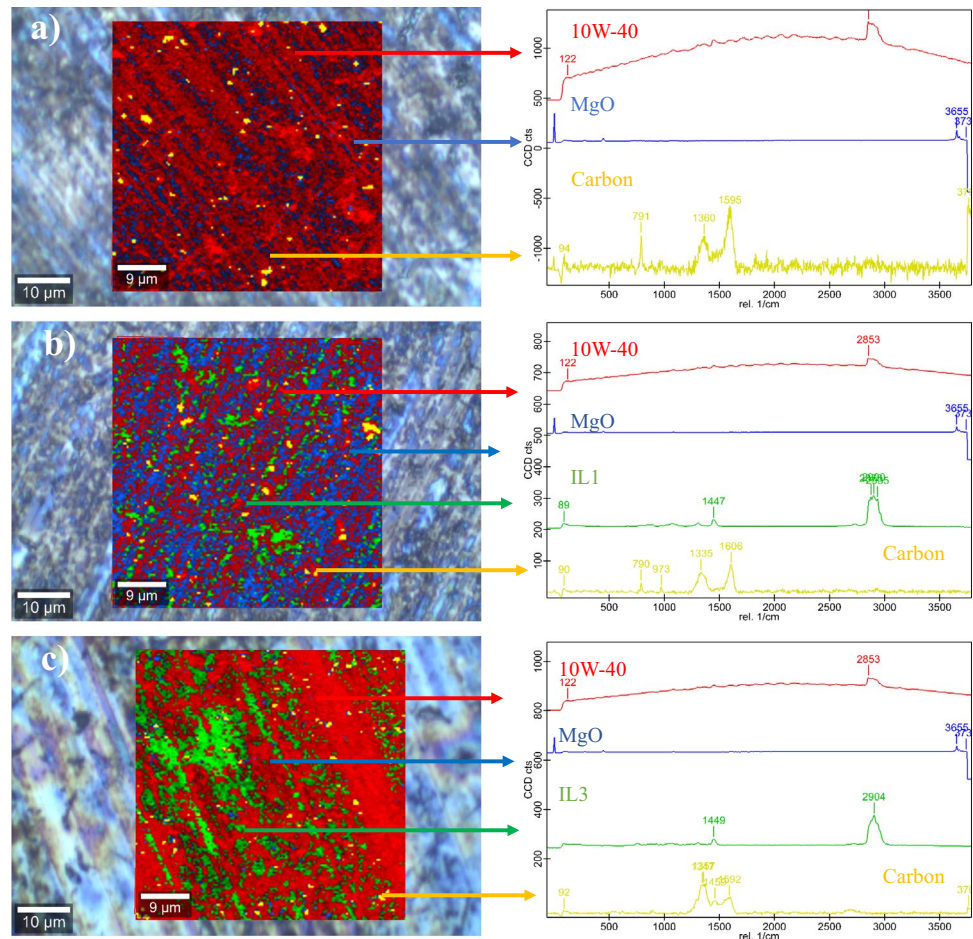
From the wear generated by friction tests, wear volume reductions, and cross-sectional profiles of worn tracks on lubricated pins are exhibited in Figs. 11 and 12, respectively. The WTW, WTD, worn area and volume values gotten from worn tracks on the surface of the pins lubricated with each formulated lubricant and 10W-40 oil are shown in Table 1. It can be underlined that for the MgO nanolubricants (hybrid and non-hybrid), the generated wear in pins is smaller than for the 10W-40 oil for all parameters (WTW, WTD, area and volume). Specifically, the highest wear area reduction was reached with 10W-40 + 0.01 wt% MgO + 1 wt% IL3 hybrid nanolubricant leading to a 24% decrease, corresponding to a 59% reduction in wear volume. Therefore, this result is in line with the highest friction reduction achieved with the same IL3-based hybrid nanolubricant. The results obtained for the wear parameters when an ionic liquid alone (IL1 or IL3) was added to the engine oil showed an increase in WTW, WTD, area and volume, which is consistent with the results obtained for the coefficient of friction, which also increased compared to that obtained with the unaltered 10W-40.

Figure 12 reveals that the wear track profile for the steel-to-steel contact lubricated with the IL3 hybrid nanolubricant

Table 2 Mean roughness data, Ra, and their uncertainties, σ , inside the worn tracks lubricated with tested 10W-40 lubricants make use of a Gaussian filter (0.025 mm cut-off)

Lubricant	Ra/nm	σ
10W-40	80.0	1.0
+0.01 wt% MgO	54.6	2.2
+0.01 wt% MgO + 1 wt% IL1	74.5	0.6
+0.01 wt% MgO + 1 wt% IL3	79.3	1.2

Fig. 13 Raman mapping and spectra inside the wear scar lubricated with formulated oil additivated with **a** 0.01 wt% MgO, **b** 0.01 wt% MgO and 1 wt% IL1 and **c** 0.01 wt% MgO and 1 wt% IL3



has a shallower wear track depth (WTD) than the contact lubricated with the unmodified commercial oil. As already shown in Table 1, there is a 32% reduction in WTD obtained with the IL3 hybrid nanolubricant compared to that produced by the 10W-40 oil.

Roughness (R_a) within the worn pins' tops was analysed to study the anti-wear nanolubricant and hybrid nanolubricants capability. Table 2 shows that worn tracks lubricated with all the tested samples have minor R_a values than those of 10W-40 oil. Precisely, a R_a value of 80.0 nm was attained in the 10W-40 worn track whereas for the scar lubricated with the 10W-40 + 0.01 wt% MgO nanolubricant, the littlest R_a value (54.6 nm) was achieved implying a roughness drop of 32%. However, the decrease in roughness for the hybrid nanolubricants (IL1 and IL3) is almost negligible. This fact can be explained because the main wear mechanism that occurs when the nanoadditive (MgO) is used stand-alone is the polishing effect. This effect has also been reported by Loo et al. [18] for MgO nanoparticles as lubricant additives to a base-blended fuel. The polishing effect is cancelled out by the addition of ionic liquids.

3.3 Worn Surface and Effect of Hybrid Combination

Elemental mapping and Raman spectra of the worn tracks on AISI 52100 (100Cr6) pins tested with 10W-40 lubricants additivated with MgO with or without IL were carried out by means of a confocal Raman microscope (532 nm) to gain a further insight into the tribo-chemical reactions between the MgO-IL-formulated oil blends and steel substrate inside the wear scar. Raman spectra of the different components were previously reported: 10W-40 and MgO nanopowders (Sect. 2.1) while IL1 and IL3 in Fig. S1 of supporting information of Nasser et al. [29]. Figure 13a, b and c shows the Raman imaging and spectra inside the wear track after a test lubricated with MgO nanolubricant, MgO + IL1- and MgO + IL3-based hybrid nanolubricants, respectively.

From the Raman mapping, the presence of MgO (Fig. 13a) and ILs (Fig. 13b and c) tribo films can be clearly detected. The characteristic bands at 281 and 446 cm^{-1} corresponding to MgO spectra (Fig. 4) were detected inside the wear scars (blue colour) for the three samples. In addition, the Raman spectra obtained inside the wear track exhibited carbon deposition when the steel substrate was lubricated

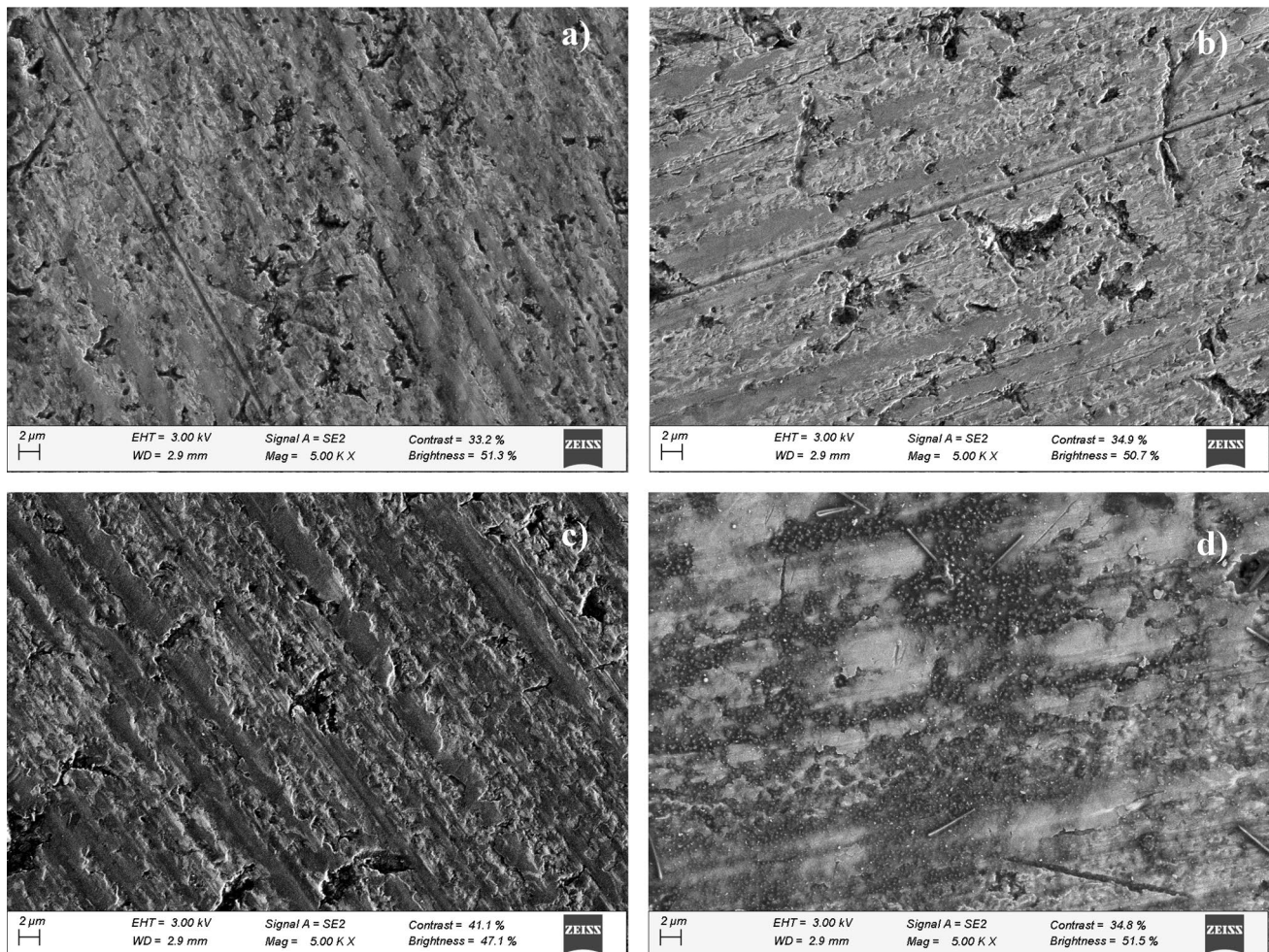


Fig. 14 SEM images inside of the wear scars on the steel discs from the test lubricated with: **a** 10W-40 engine oil, **b** 0.01 wt% MgO, **c** 0.01 wt% MgO and 1 wt% IL1 and **d** 0.01 wt% MgO and 1 wt% IL3

with MgO, MgO + 1 wt% IL1 and MgO + 1 wt% IL3. The solid yellow curve represents this spectrum detected from the region marked with yellow points. Very strong peaks corresponding to D and G bands were found around 1340 and 1590 cm^{-1} , which can be attributed to the graphite structures formed on steel surfaces due to the decomposition of the hydrocarbon radicals that are in agreement with the values in the literature [42]. When formulated oil was only added with MgO on steel surface, the hydrocarbon decomposition also occurred inside the wear track as can be seen from the yellow spectrum in Fig. 13a in addition to a predominant presence of formulated oil (red colour). The compounds generated on top of the steel surface further confirmed the formation of tribo-film when the ILs are used (green colour), especially with the use of IL3 as an additive. These results may explain why the presence of IL3 enhanced the wear resistance of 10W-40 oil in Figs. 11 and 12 to a

greater extent illustrating the positive anti-wear synergies found between IL3 and MgO as hybrid additives. In addition, Fig. 13a illustrates the concentration distribution of MgO on the worn surface as a single additive to 10W-40 engine oil. This distribution concentration was increased when IL1 was added as indicated in Fig. 13b. The friction coefficient generally rises with increase in concentration of additives in engine oil and may be referred to transient agglomeration of the nanoparticles on the surface [19]. So, the reduction of friction and wear in the case of MgO/IL1 could be referred to the lubricity of IL1 and the impact of its anion [DEHP]. In the case of the addition of IL3, homogeneous distribution of both MgO and IL3 was detected. The anion $[(iC8)_2PO_2]$ of IL3 could be the main reason to prevent extra agglomeration and proper surface distribution of MgO nanopowders on the worn surface. This nanoadditives distribution enhancement generated by IL3 was also

Table 3 EDX analysis of worn surface of steel pins tested with 10W-40 engine oil, MgO nanolubricant and IL1 and IL3 hybrid nanolubricants

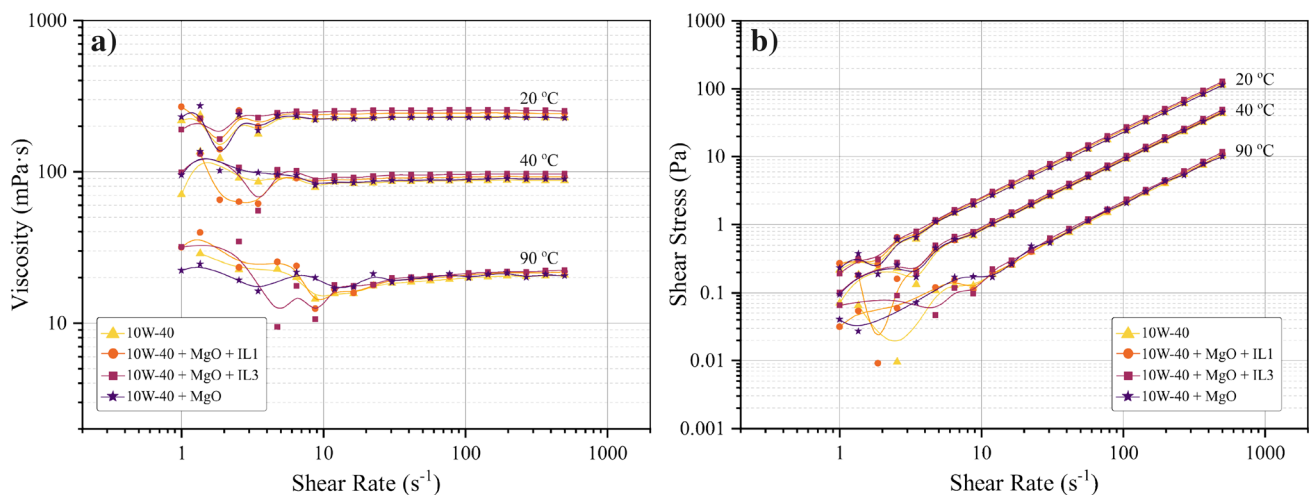
Elemental composition	10W-40	+0.01 wt% MgO	+0.01 wt% MgO + 1 wt% IL1	+0.01 wt% MgO + 1 wt% IL3
C	10.21	7.56	6.77	11.77
O	1.58	2.12	2.18	2.61
Mg	–	–	0.03	–
Al	0.10	0.09	0.12	0.10
Si	1.55	1.22	1.13	0.71
P	0.25	0.43	0.48	0.50
S	0.29	0.40	0.35	0.61
Ca	0.15	0.23	0.36	0.35
Cr	1.40	1.49	1.40	1.27
Mn	0.29	0.37	0.30	0.27
Fe	83.72	85.38	86.15	81.22
Zn	0.47	0.71	0.70	0.59
Cd	–	–	0.02	–
Total	100.00	100.00	100.00	100.00

observed in previous studies when the combination of IL3/graphene nanoplatelets/hexagonal boron nitride was studied as double hybrid additives [48]. This agrees with the wear volume reduction shown in Table 1, with MgO + 1 wt% IL3 having the highest anti-wear capacity (59%) among the other samples.

To better understand the anti-wear mechanisms of the nanoparticles in the commercial oil and to know the composition of the possible tribo-film, the wear scar of the tested steel pins was scanned and analysed by SEM–EDX. Figure 14a–d shows the 5000X scanned SEM images of the wear scar of the tested steel pins for the formulated engine

oil, the MgO nanolubricant and the hybrid nanolubricants based on IL1 and IL3. Figure 14a reveals severe cracking and pitting on the worn surface lubricated with the 10W-40 engine oil. Whereas the SEM image of the wear scar with the MgO nanolubricant shows a smoother wear scar surface, thus confirming the polishing effect deduced from the roughness measurements, deep cracks are still observed, so MgO does not seem to perform a repairing effect. With the addition of IL1 and MgO to the engine oil, the surface is rougher, so the polishing effect produced by MgO in the previous case disappears with the addition of IL1, and the cracks remain again on the surface of the track but with an irregular groove (Fig. 14c). However, with the addition of IL3 and MgO, a smoother surface was observed, hardly any pitting was found, and the grooves are very fine compared to the abraded surface lubricated with the engine oil, as shown in Fig. 14d. The cracks are not visible, because they are filled with spherical clusters and discontinuous films are visible in the sliding direction. This indicates that the addition of the MgO + IL3 mixture enhanced the anti-wear effects of the commercial oil by the repair mechanism (as the MgO nanoparticles tend to fill the surface imperfections) and by IL3 protective film formation.

Finally, to know the composition inside the worn surface of the tested steel pins, an elemental energy-dispersive X-ray (EDX) analysis was performed on the contacts lubricated with formulated engine oil, with the MgO nanolubricant and with the hybrid nanolubricants based on IL1 and IL3. Table 3 shows the elemental composition detected for each sample. EDX results revealed that up to thirteen types of elements were found on the worn surfaces of the steel pins tested. The most abundant element (81–86 wt%) detected in each sample was iron (Fe), which is expected as it is the main element in the 100Cr6

**Fig. 15** a Viscosity and b Shear Stress of the four samples versus shear rate at different temperatures. $T=293.15, 313.15$ and 363.15 K

steel pin. The carbon (C), chromium (Cr), manganese (Mn) and silicon (Si) also come from the 100Cr6 steel pin [49]. C is the second element with the highest percentage by weight in each sample, which may be due to the fact that it can also come from the used 10W-40 engine oil. Other elements detected such as sulphur (S), zinc (Zn), phosphorus (P) and calcium (Ca) are typical additives of 10W-40 engine oil [50, 51]. The oxygen (O) element can be related to the oxide-protective layer formed on the worn surface during the friction process. The addition of the MgO nanoparticle additive in the engine oil increases the oxygen content, which results in the formation of a more resistant oxide layer on the contact surface, providing better wear protection [18]. The higher oxygen content is observed in the wear scar of the IL3 hybrid nanolubricant, thus confirming the excellent wear performance observed in Fig. 11. Magnesium (Mg) element has only been detected in very low composition on the contact surface lubricated with the IL1 hybrid nanolubricant. The difficulty in detecting Mg is due to the low concentration used as an additive (0.01 wt%).

3.4 Rheological Behaviour

The rheological characterization for the three samples: 0.01 wt% MgO/10W-40, 0.01 wt% MgO-IL1/10W-40 and 0.01 wt% MgO-IL3/10W-40 was performed and compared to that of the neat engine oil in efforts to quantify the viscosity and evaluate the rheological behaviour of the nanolubricant and hybrid nanolubricants. Figure 15 shows the results. From the obtained data, it can be noted that the inclusion of nanoparticles and ILs slightly enhances the viscosity of the commercial oil. This response is consistent with that reported in previous studies on similar systems [29] and it can be explained by the fact that the Brownian motion of nanoparticles draws them closer together, resulting in nanoparticle collision. Due to Van der Waals forces, the nanoparticles attract each other, form clusters and, eventually, may also cause the gelation of the ionic liquid [11]. However, in the present case, the differences in viscosity are so feeble that is safe to assume that the movement of fluid layers over each other will not be affected by these subtle variations, allowing the layers to glide freely despite the presence of additives. Figure 15 also shows the temperature influence in the rheological parameters. As expected, when the temperature rises, intermolecular interactions in nanoparticles and base fluid molecules reduce, resulting in a drop in nanofluid viscosity. For this particular case, viscosity values at 293.15 K are of the order of 200 mPa s^{-1} , and when the temperatures reach 363.15 K, dynamic viscosity diminish to values under 20 mPa s^{-1} , which means a reduction of over 90%. Nonetheless, this temperature dependence can be partially controlled by modifying the nanoparticle

concentration. It has been demonstrated that nanoclusters which prevent the movement of oil layers on each other have a higher impact on the lubricant viscosity when temperatures are low, due to the fact that the rise in temperature helps the particles to overcome the attractive van der Waals forces [52]. Consequentially, lubricants with a higher nanoparticle concentration would experiment a more sensible response at temperature changes.

Besides, from the viscosity and shear stress plots, it is also possible to deduce the flow behaviour of the nanolubricants. The four samples presented a linear relation between shear stress and shear rate, and the viscosity values remained constant through all the range studied. From that, it can be safely inferred that all studied nanofluids behave as Newtonian, which is a critical condition for their use in applications where convective heat transfer takes place, such as internal combustion engines [52].

4 Conclusions

The tribological and rheological properties as well as the stability of the certain concentration (1 wt%) of different trihexyltetradecylphosphonium-based ionic liquids and magnesium oxide nanoparticles (0.01 wt%) were investigated. The results indicate that the addition of MgO nanoparticles dispersed in the ionic liquid in the formulated lubricant can outperform the tribological performance of the stand-alone lubricant. In particular, it was found that concentrations of 0.01 wt% and 1 wt% for the nanoparticles and for the IL3, respectively, were optimal in terms of providing the best anti-wear properties for steel/steel contact, achieving 59% reduction in wear volume. Moreover, no sedimentation was detected for all the formulated lubricants up to three weeks after their preparation. The improvement in the tribological properties was attributed to the following: (i) the formation of a protective tribo-film; (ii) the ability of nanoparticles to fill out valleys between asperities, thereby effectively smoothing out the shearing surfaces. Furthermore, in relation to the influence of MgO nanoparticles and phosphonium-based ILs on the rheological behaviour of the formulated 10W-40 commercial oil, it is observed that they do not produce any change on its Newtonian behaviour, the viscosity remaining unchanged at different shear rates. In essence, this study has shown that the addition of ionic liquids to MgO nanoparticles can improve the stability and lubrication behaviour of MgO nanolubricant and encourages more investigations on using nanoparticle additives with green solvents such as ionic liquids to protect the environment as well as prolong the lifetime of machinery.

Acknowledgements The authors are grateful to REPSOL partners for the advice and for providing us the sample of formulated oil studied

in this work. We would also like to thank the use of RIAIDT-USC analytical facilities.

Author Contributions JMLdR and MJGG contributed to conceptualization, provided methodology and wrote the main manuscript text. RR provided methodology and wrote the section on Rheological behaviour. KN completed the sections Friction and Wear and Worn Surface and Effect of Hybrid Combination. All authors contributed to reviewing and editing of the manuscript.

Funding This research is part of the project ENE2017-86425-C2-1/2-R funded by MCIN/AEI/10.13039/501100011033 and by ERDF “A way of making Europe” and has also been supported through the GRC grant ED431C 2020/10 by the Xunta de Galicia. Dr. M.J.G.G. acknowledges a postdoctoral fellowship (ED481B-2019-015) from the Xunta de Galicia (Spain). Dr. J.M.L.dR and Dr. R.R. are grateful for financial support through the Margarita Salas programme, funded by MCIN/AEI/10.13039/501100011033 and “NextGenerationEU/PRTR”. Open Access funding provided thanks to the CRUE-CSIC agreement with Springer Nature.

Declarations

Competing interest The authors declare no competing interests.

Open Access This article is licensed under a Creative Commons Attribution 4.0 International License, which permits use, sharing, adaptation, distribution and reproduction in any medium or format, as long as you give appropriate credit to the original author(s) and the source, provide a link to the Creative Commons licence, and indicate if changes were made. The images or other third party material in this article are included in the article's Creative Commons licence, unless indicated otherwise in a credit line to the material. If material is not included in the article's Creative Commons licence and your intended use is not permitted by statutory regulation or exceeds the permitted use, you will need to obtain permission directly from the copyright holder. To view a copy of this licence, visit <http://creativecommons.org/licenses/by/4.0/>.

References

- Davis, D., Shah, A.F., Panigrahi, B.B., Singh, S.: Effect of Cr₂AlC nanolamella addition on tribological properties of 5W–30 engine oil. *Appl. Surf. Sci.* **493**, 1098–1105 (2019). <https://doi.org/10.1016/j.apsusc.2019.07.097>
- Waqas, M., Zahid, R., Bhutta, M.U., Khan, Z.A., Saeed, A.: A review of friction performance of lubricants with nano additives. *Materials* **14**, 6310 (2021). <https://doi.org/10.3390/ma14216310>
- Kamel, B.M., Tirth, V., Algahtani, A., Shiba, M.S., Mobasher, A., Hashish, H.A., Dabees, S.: Optimization of the rheological properties and tribological performance of SAE 5W–30 base oil with added MWCNTs. *Lubricants* **9**, 94 (2021). <https://doi.org/10.3390/lubricants9090094>
- Ali, M.K.A., Xianjun, H., Turkson, R.F., Peng, Z., Chen, X.: Enhancing the thermophysical properties and tribological behaviour of engine oils using nano-lubricant additives. *RSC Adv.* **6**, 77913–77924 (2016). <https://doi.org/10.1039/C6RA10543B>
- Nobrega, G., de Souza, R.R., Gonçalves, I.M., Moita, A.S., Ribeiro, J.E., Lima, R.A.: Recent developments on the thermal properties, stability and applications of nanofluids in machining, solar energy and biomedicine. *Appl. Sci.* **12**, 1115 (2022). <https://doi.org/10.3390/app12031115>
- Tang, Z., Li, S.: A review of recent developments of friction modifiers for liquid lubricants (2007–present). *Curr. Opin. Solid State Mater. Sci.* **18**, 119–139 (2014). <https://doi.org/10.1016/j.cossms.2014.02.002>
- Nadooshan, A.A., Esfe, M.H., Afrand, M.: Evaluation of rheological behavior of 10W40 lubricant containing hybrid nano-material by measuring dynamic viscosity. *Phys. E* **92**, 47–54 (2017). <https://doi.org/10.1016/j.physe.2017.05.011>
- Khan, I., Saeed, K., Khan, I.: Nanoparticles: properties, applications and toxicities. *Arab. J. Chem.* **12**, 908–931 (2019). <https://doi.org/10.1016/j.arabjc.2017.05.011>
- Guo, D., Xie, G., Luo, J.: Mechanical properties of nanoparticles: basics and applications. *J. Phys. D* **47**, 13001 (2013). <https://doi.org/10.1088/0022-3727/47/1/013001>
- Shahnazar, S., Bagheri, S., Hamid, S.B.A.: Enhancing lubricant properties by nanoparticle additives. *Int. J. Hydrog. Energy* **41**, 3153–3170 (2016). <https://doi.org/10.1016/j.ijhydene.2015.12.040>
- Shafi, W.K., Charoo, M.S.: An overall review on the tribological, thermal and rheological properties of nanolubricants. *Tribol. Mater. Surf. Interfaces* **15**, 20–54 (2021). <https://doi.org/10.1080/17515831.2020.1785233>
- Wu, Y.Y., Tsui, W.C., Liu, T.C.: Experimental analysis of tribological properties of lubricating oils with nanoparticle additives. *Wear* **262**, 819–825 (2007). <https://doi.org/10.1016/j.wear.2006.08.021>
- Battez, A.H., González, R., Viesca, J.L., Fernández, J.E., Fernández, J.M.D., Machado, A., Chou, R., Riba, J.: CuO, ZrO₂ and ZnO nanoparticles as antiwear additive in oil lubricants. *Wear* **265**, 422–428 (2008). <https://doi.org/10.1016/j.wear.2007.11.013>
- Battez, A.H., González, R., Felgueroso, D., Fernández, J.E., del Fernández, M., García, M.A.R., Peñuelas, I.: Wear prevention behaviour of nanoparticle suspension under extreme pressure conditions. *Wear* **263**, 1568–1574 (2007). <https://doi.org/10.1016/j.wear.2007.01.093>
- Ingole, S., Charanpahari, A., Kakade, A., Umare, S.S., Bhatt, D.V., Menghani, J.: Tribological behavior of nano TiO₂ as an additive in base oil. *Wear* **301**, 776–785 (2013). <https://doi.org/10.1016/j.wear.2013.01.037>
- Kotia, A., Ghosh, G.K., Srivastava, I., Deval, P., Ghosh, S.K.: Mechanism for improvement of friction/wear by using Al₂O₃ and SiO₂/Gear oil nanolubricants. *J. Alloys Compd.* **782**, 592–599 (2019). <https://doi.org/10.1016/j.jallcom.2018.12.215>
- Singh, Y., Badhotiya, G.K., Gwalwanshi, M., Negi, P., Bist, A.: Magnesium oxide (MgO) as an additive to the neem oil for efficient lubrication. *Mater. Today: Proc.* **46**, 10478–10481 (2021). <https://doi.org/10.1016/j.matpr.2020.12.1181>
- Loo, D.L., Teoh, Y.H., How, H.G., Le, T.D., Nguyen, H.T., Rashid, T., Pottmaier, D., Sher, F.: Effect of nanoparticles additives on tribological behaviour of advanced biofuels. *Fuel* **334**, 126798 (2023). <https://doi.org/10.1016/j.fuel.2022.126798>
- Vadiraj, A., Manivasagam, G., Kamani, K., Sreenivasan, V.S.: Effect of nano oil additive proportions on friction and wear performance of automotive materials. *Tribol. Ind.* **34**, 3–10 (2012)
- Gulzar, M., Masjuki, H.H., Kalam, M.A., Varman, M., Zulkifli, N.W.M., Mufti, R.A., Zahid, R.: Tribological performance of nanoparticles as lubricating oil additives. *J. Nanoparticle Res.* **18**, 223 (2016). <https://doi.org/10.1007/s11051-016-3537-4>
- Mungse, H.P., Khatri, O.P.: Chemically functionalized reduced graphene oxide as a novel material for reduction of friction and wear. *J. Phys. Chem. C* **118**, 14394–14402 (2014). <https://doi.org/10.1021/jp5033614>
- Zhang, Z.J., Simionesie, D., Schaschke, C.: Graphite and hybrid nanomaterials as lubricant additives. *Lubricants* **2**, 44–65 (2014). <https://doi.org/10.3390/lubricants2020044>

23. Somers, A.E., Howlett, P.C., MacFarlane, D.R., Forsyth, M.: A review of ionic liquid lubricants. *Lubricants* **1**, 3–21 (2013). <https://doi.org/10.3390/lubricants1010003>
24. Zhou, Y., Qu, J.: Ionic liquids as lubricant additives: a review. *ACS Appl. Mater. Interfaces* **9**, 3209–3222 (2017). <https://doi.org/10.1021/acsami.6b12489>
25. Bermúdez, M.-D., Jiménez, A.-E., Sanes, J., Carrión, F.-J.: Ionic liquids as advanced lubricant fluids. *Molecules* **14**, 2888–2908 (2009). <https://doi.org/10.3390/molecules14082888>
26. Cai, M., Yu, Q., Liu, W., Zhou, F.: Ionic liquid lubricants: when chemistry meets tribology. *Chem. Soc. Rev.* **49**, 7753–7818 (2020). <https://doi.org/10.1039/D0CS00126K>
27. Ali, M.K.A., Abdelkareem, M.A.A., Chowdary, K., Ezzat, M.F., Kotia, A., Jiang, H.: A review of recent advances of ionic liquids as lubricants for tribological and thermal applications. *Proc. Inst. Mech. Eng. J.* **237**, 3–26 (2023). <https://doi.org/10.1177/13506501221091133>
28. Qu, J., Luo, H., Chi, M., Ma, C., Blau, P.J., Dai, S., Viola, M.B.: Comparison of an oil-miscible ionic liquid and ZDDP as a lubricant anti-wear additive. *Tribol. Int.* **71**, 88–97 (2014). <https://doi.org/10.1016/j.triboint.2013.11.010>
29. Nasser, K.I., del Río, J.M.L., López, E.R., Fernández, J.: Synergistic effects of hexagonal boron nitride nanoparticles and phosphonium ionic liquids as hybrid lubricant additives. *J. Mol. Liq.* **311**, 113343 (2020). <https://doi.org/10.1016/j.molliq.2020.113343>
30. Alirezaie, A., Saedodin, S., Esfe, M.H., Rostamian, S.H.: Investigation of rheological behavior of MWCNT (COOH-functionalized)/MgO - Engine oil hybrid nanofluids and modelling the results with artificial neural networks. *J. Mol. Liq.* **241**, 173–181 (2017). <https://doi.org/10.1016/j.molliq.2017.05.121>
31. Kotia, A., Chowdary, K., Srivastava, I., Ghosh, S.K., Ali, M.K.A.: Carbon nanomaterials as friction modifiers in automotive engines: recent progress and perspectives. *J. Mol. Liq.* (2020). <https://doi.org/10.1016/j.molliq.2020.113200>
32. Praveena, M., Guha, K., Ravishankar, A., Biswas, S.K., Bain, C.D., Jayaram, V.: Total internal reflection Raman spectroscopy of poly(alpha-olefin) oils in a lubricated contact. *RSC Adv.* **4**, 22205–22213 (2014). <https://doi.org/10.1039/C4RA02261K>
33. Okubo, H., Tadokoro, C., Hirata, Y., Sasaki, S.: In situ raman observation of the graphitization process of tetrahedral amorphous carbon diamond-like carbon under boundary lubrication in poly-alpha-olefin with an organic friction modifier. *Tribol Online* **12**, 229–237 (2017). <https://doi.org/10.2474/trol.12.229>
34. Iolitec, <https://nanomaterials.iolitec.de/en/products/oxides/NO-0012-UP>, 2022 Accessed 13 July 2022
35. Balakrishnan, G., Velavan, R., Batoo, K.M., Raslan, E.H.: Microstructure, optical and photocatalytic properties of MgO nanoparticles. *Results Phys.* **16**, 103013 (2020). <https://doi.org/10.1016/j.rinp.2020.103013>
36. Balamurugan, S., Ashna, L., Parthiban, P.: Synthesis of Nanocrystalline MgO Particles by Combustion Followed by Annealing Method Using Hexamine as a Fuel. *J. Nanotechnol.* **2014**, 841803 (2014). <https://doi.org/10.1155/2014/841803>
37. Selvam, N.C.S., Kumar, R.T., Kennedy, L.J., Vijaya, J.J.: Comparative study of microwave and conventional methods for the preparation and optical properties of novel MgO-micro and nano-structures. *J. Alloys Compd.* **509**, 9809–9815 (2011). <https://doi.org/10.1016/j.jallcom.2011.08.032>
38. Krishnamoorthy, K., Moon, J.Y., Hyun, H.B., Cho, S.K., Kim, S.-J.: Mechanistic investigation on the toxicity of MgO nanoparticles toward cancer cells. *J. Mater. Chem.* **22**, 24610–24617 (2012). <https://doi.org/10.1039/C2JM35087D>
39. Kim, H.S., Kim, H.W.: Fabrication and Raman Studies omicrf MgO/SnO₂ Core Shell Heteronanowires. *Acta Phys. Pol. A* **116**, 58–61 (2009). <https://doi.org/10.12693/APhysPolA.116.58>
40. Karthik, K., Dhanuskodi, S., Gobinath, C., Prabukumar, S., Sivaramkrishnan, S.: Fabrication of MgO nanostructures and its efficient photocatalytic, antibacterial and anticancer performance. *J. Photochem. Photobiol. B* **190**, 8–20 (2019). <https://doi.org/10.1016/j.jphotobiol.2018.11.001>
41. Wahab, R., Ansari, S.G., Dar, M.A., Kim, Y.S., Shin, H.S.: Synthesis of Magnesium Oxide Nanoparticles by Sol-Gel Process. *Mater. Sci. Forum* **558–559**, 983–986 (2007). <https://doi.org/10.4028/www.scientific.net/MSF.558-559.983>
42. del Liñeira, J.M.R., López, E.R., Fernández, J.: Synergy between boron nitride or graphene nanoplatelets and tri(butyl)ethylphosphonium diethylphosphate ionic liquid as lubricant additives of triisotridecyltrimellitate oil. *J. Mol. Liq.* **301**, 112442 (2020). <https://doi.org/10.1016/j.molliq.2020.112442>
43. Sanes, J., Avilés, M.-D., Saurín, N., Espinosa, T., Carrión, F.-J., Bermúdez, M.-D.: Synergy between graphene and ionic liquid lubricant additives. *Tribol. Int.* **116**, 371–382 (2017). <https://doi.org/10.1016/j.triboint.2017.07.030>
44. Kawada, S., Watanabe, S., Tsuboi, R., Sasaki, S., Prakash, B.: Lubrication mechanism of halogen-free ionic liquids. *Tribol. Online* **12**, 155–161 (2017). <https://doi.org/10.2474/trol.12.155>
45. Heyer, P., Lauger, J.: Correlation between friction and flow of lubricating greases in a new tribometer device. *Lubr. Sci.* **21**, 253–268 (2009). <https://doi.org/10.1002/ls.88>
46. Panda, A., Sahoo, A.K., Kumar, R., Das, R.K.: A review on machinability aspects for AISI 52100 bearing steel. *Mater. Today: Proc.* **23**, 617–621 (2020). <https://doi.org/10.1016/j.matpr.2019.05.422>
47. Delprete, C., Razavykia, A.: Piston dynamics, lubrication and tribological performance evaluation: a review. *Int. J. Engine Res.* **21**, 725–741 (2020). <https://doi.org/10.1177/1468087418787610>
48. Nasser, K.I., del Liñeira, J.M.R., Mariño, F., López, E.R., Fernández, J.: Double hybrid lubricant additives consisting of a phosphonium ionic liquid and graphene nanoplatelets/hexagonal boron nitride nanoparticles. *Tribol. Int.* **163**, 107189 (2021). <https://doi.org/10.1016/j.triboint.2021.107189>
49. Kiranbabu, S., Tung, P.Y., Sreekala, L., Prithiv, T.S., Hickel, T., Pippin, R., Morsdorf, L., Herbig, M.: Cementite decomposition in 100Cr6 bearing steel during high-pressure torsion: influence of precipitate composition, size, morphology and matrix hardness. *Mater. Sci. Eng. A.* **833**, 142372 (2022). <https://doi.org/10.1016/j.msea.2021.142372>
50. Amann, T., Kailer, A.: Ultralow friction of mesogenic fluid mixtures in tribological reciprocating systems. *Tribol. Lett.* **37**, 343–352 (2010). <https://doi.org/10.1007/s11249-009-9527-2>
51. Faruck, A.A.M., Hsu, C.-J., Doerr, N., Weigand, M., Gachot, C.: How lubricant formulations and properties influence the performance of rotorcraft transmissions under loss of lubrication conditions. *Tribol. Int.* **151**, 106390 (2020). <https://doi.org/10.1016/j.triboint.2020.106390>
52. Afrand, M., Najafabadi, K.N., Akbari, M.: Effects of temperature and solid volume fraction on viscosity of SiO₂-MWCNTs/SAE40 hybrid nanofluid as a coolant and lubricant in heat engines. *Appl. Therm. Eng.* **102**, 45–54 (2016). <https://doi.org/10.1016/j.applthermaleng.2016.04.002>

Publisher's Note Springer Nature remains neutral with regard to jurisdictional claims in published maps and institutional affiliations.